Science of the Total Environment 634 (2018) 1352–1361

Contents lists available at ScienceDirect

Science of the Total Environment

journal homepage: www.elsevier.com/locate/scitotenv

Dual role of DOM in a scenario of global change on photosynthesis and structure of coastal phytoplankton from the South Atlantic Ocean

Virginia E. Villafañe [a,b,*], Joanna Paczkowska [c], Agneta Andersson [c], Cristina Durán Romero [a], Macarena S. Valiñas [a,b], E. Walter Helbling [a,b]

[a] Estación de Fotobiología Playa Unión, Casilla de Correos N°15, 9103 Rawson, Chubut, Argentina
[b] Consejo Nacional de Investigaciones Científicas y Técnicas (CONICET), Argentina
[c] Department of Ecology and Environmental Science, Umeå University, 901 87 Umeå, Sweden

HIGHLIGHTS

- In a future scenario, attenuation by DOM outcompetes its physico-chemical role.
- Global change conditions will favor growth and photosynthesis of nanoplankton.
- Global change favors growth and photosynthesis of nano- as compared to microplankton.

GRAPHICAL ABSTRACT

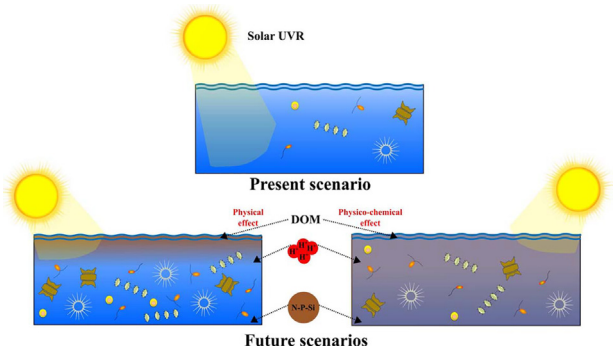

ARTICLE INFO

Article history:
Received 20 February 2018
Received in revised form 8 April 2018
Accepted 9 April 2018
Available online xxxx

Editor: Jay Gan

Keywords:
Acidification
Dissolved organic matter
Nutrients
Oxygen evolution
Photosynthesis
Ultraviolet radiation

ABSTRACT

We evaluated the dual role of DOM (i.e., as a source of inorganic nutrients and as an absorber of solar radiation) on a phytoplankton community of the western South Atlantic Ocean. Using a combination of microcosms and a cluster approach, we simulated the future conditions of some variables that are highly influenced by global change in the region. We increased nutrients (i.e., anthropogenic input) and dissolved organic matter (DOM), and we decreased the pH, to assess their combined impact on growth rates (μ), species composition/abundance and size structure, and photosynthesis (considering in this later also the effects of light quality i.e., with and without ultraviolet radiation). We simulated two Future conditions (Fut) where nutrients and pH were similarly manipulated, but in one the physical role of DOM (Fut_{out}) was assessed whereas in the other (Fut_{in}) the physico-chemical role was evaluated; these conditions were compared with a control (Present condition, Pres). The μ significantly increased in both Fut conditions as compared to the Pres, probably due to the nutrient addition and acidification in the former. The highest μ were observed in the Fut_{out}, due to the growth of nanoplanktonic flagellates and diatoms. Cells in the Fut_{in} were photosynthetically less efficient as compared to those of the Fut_{out} and Pres, but these physiological differences, also between samples with or without solar UVR observed at the beginning of the experiment, decreased with time hinting for an acclimation process. The knowledge of the relative importance of both roles of DOM is especially important for coastal areas that are expected to receive higher inputs and will be more acidified in the future.

* Corresponding author at: Estación de Fotobiología Playa Unión, Casilla de Correos N°15, 9103 Rawson, Chubut, Argentina.
E-mail addresses: virginia@efpu.org.ar, (V.E. Villafañe), agneta.andersson@umu.se, (A. Andersson), mval@efpu.org.ar, (M.S. Valiñas), whelbling@efpu.org.ar. (E.W. Helbling).

https://doi.org/10.1016/j.scitotenv.2018.04.121
0048-9697/

1. Introduction

Coastal areas are highly productive ecosystems contributing for a large share of the World's aquatic primary productivity (Cloern et al., 2014) and providing countless ecosystemic services (e.g., processing of nutrients and of pollutants, accumulating and storing carbon, and also constituting refuge and nursery areas that support secondary production, UNEP, 2006; Canuel et al., 2012). The increasing human population and changes in land use along coastal areas have been the main source of high amounts of nutrients, as well as of sewage and toxic elements coming into the water, altering the physical, chemical and biological environment (UNEP, 2006; Rabalais et al., 2009; Cloern et al., 2016). In addition, increased rainfall carries high amounts of terrigenous material, both in the form of particulate (organic and inorganic) and dissolved organic matter (DOM) (Häder et al., 2014) that are then incorporated in the water column. These materials (defined arbitrarily by their size) are a mixture of several autochthonous and allochthonous components (e.g., humic and fulvic acids, smaller molecules like amino acids and carbohydrates) that have a dual ecological role: on the one hand, they are nutrient sources for heterotrophic and autotrophic organisms (Jones, 1992; Traving et al., 2017); on the other hand, they act as absorbers of solar radiation, decreasing the underwater radiation field (Santos et al., 2016). This dual role results in both, positive and negative effects on phytoplankton, such that increased amounts of DOM favored the growth of phytoplankton communities (Klug, 2002) or of the diatom *Asterionella formosa* (Kissman et al., 2013) due to stimulation by nutrients, whereas they inhibited phytoplankton growth (i.e., biomass) by reducing the underwater radiation (Klug, 2002; Traving et al., 2017). All these responses to single DOM effects can be synergistic- or antagonistically altered by the interaction with other global change variables (Crain et al., 2008). For example, the combined effects of increased temperatures and inputs of DOM resulted in a shift of the structure and of the relative abundances of bacterioplankton groups in the Baltic Sea that could scale up to other trophic levels i.e., phytoplankton (Lindh et al., 2015). Also the type of DOM, in combination with the input of nutrients, resulted in different growth rates favoring small phytoplankton cells (<20 μm) and bacteria in a Chilean fjord (Iriarte et al., 2014). There are also evidences that lower pH affected the amount and concentration of DOM released by phytoplankton (Riebesell, 2004; Thornton, 2014) shaping the microbial community and the biological pump as a whole by increasing the DOC/POC ratio and thus more carbon would remain in the upper ocean rather sinking out of the euphotic zone, as seen in experiments carried out in the Korean coast (Kim et al., 2011). Furthermore, studies addressing the interaction of increasing amounts of DOM with vertical mixing proved to be synergistic, resulting in a feedback mechanism by which cyanobacteria blooms would not develop in mid latitudes (Helbling et al., 2015).

Since coastal organisms, especially those inhabiting estuaries, are generally well adapted to a wide range of biological, chemical and physical conditions (Wilson, 2008) one key question is what would be their response in a global change scenario and/or under anthropogenic pressure. According to Rabalais et al. (2009) the expected changes in coastal waters e.g., higher temperatures, stronger stratification and increased inflows of freshwater and nutrients, will result in enhanced production and growth of phytoplankton and macroalgae. In fact, experiments using microcosms and simulated in situ conditions in Patagonian waters - in which nutrients, solar radiation and acidification have been manipulated, agree with this view (Villafañe et al., 2015; Durán-Romero et al., 2017) although it is not possible to extrapolate these results if more variables are added.

The coastal South Atlantic area receives high inputs of terrigenous material from riverine origin, which brings also nutrients from anthropogenic-related activities such as agriculture and fishing (Bermejo et al., 2018). In addition, the Patagonian dust, which carries micronutrients such as Fe (Johnson et al., 2011) and other nutrients, can significantly affect the biological activity (i.e., photosynthesis and respiration) of phytoplankton (Cabrerizo et al., 2017). Therefore, it is of great importance to evaluate the role that the terrigenous material has on the lower levels of the aquatic food web. Moreover, in a scenario of global change it is expected, for coastal areas, an increase of DOM due to higher precipitation that promotes greater run off (Häder et al., 2015). In this case, these areas will receive more nutrients, and it will also be turned towards darker environments. Thus we designed an experiment to test the dual role of DOM under simulated conditions of global change, using a phytoplankton community from coastal South Atlantic waters. In our experiment we evaluated separately the physical (e.g., attenuation) and the physico-chemical roles of DOM, and we assessed their relative importance when phytoplankton were acclimated to simulated future conditions of global change of increased acidity and nutrients, which are variables that we know from previous studies that have a great impact on the physiology and structure of phytoplankton in the area (Villafañe et al., 2015; Durán-Romero et al., 2017). Briefly, we set up two Future experimental scenarios that received the same amount of solar radiation, but while in one (Fut_{in}) the effects of the addition of DOM were both physical (i.e., attenuation of solar radiation) and chemical (i.e., utilization, degradation, etc.), in the other (Fut_{out}) they were only physical. We hypothesized that the physico-chemical role of DOM will enhance phytoplankton photosynthesis and growth more than the physical role alone as cells will be protected against high levels of solar radiation at the same time that they receive more nutrients. Our results will be of key importance for this rather under-sampled area of the South Atlantic Ocean – Patagonian coastal waters, which is widely recognized for its high primary and secondary productivity (Behrenfeld and Falkowski, 1997; Skewgar et al., 2007; De Carli et al., 2012).

2. Materials and methods

2.1. Study area

This study was carried out with seawater collected at the mouth of the Chubut River estuary (Chubut Province, Patagonia Argentina, 43° 20.5′ S, 65° 02.0′ W). The study area, a coastal temperate site in the South Atlantic Ocean, is characterized by a wide range of physical, chemical and biological variables, due to the interaction between the river and the sea (Helbling et al., 2010; Bermejo et al., 2018). The river also carries a heavy load of particulate and dissolved materials (Scapini et al., 2010, 2011) that strongly attenuates the penetration of solar radiation in the water column and also modifies the transparency of the coastal seawater side (Helbling et al., 2010) reaching attenuation coefficients (kd_{PAR}) as high as 6 m^{-1}. Macronutrients also have large variability during the year, with ranges 0.20–21 μM for nitrite + nitrate, 0.19–6.4 μM for phosphate, and 1.7–236 μM for silicate (Helbling et al., 2010; Bermejo et al., 2018); while phytoplankton biomass and Chl-*a* concentration had values up to ca. 550 μg C L^{-1} and 80 μg Chl-*a* L^{-1}, respectively (Bermejo et al., 2018). This coastal area is one of the most productive in the South Atlantic Ocean (Rousseaux and Gregg, 2014) and it is furnished by a continuous download of nutrients, carried by the Chubut River (Helbling et al., 2010; Bermejo et al., 2018).

2.2. Experimental set up

A surface seawater sample (ca. 200 L, from the upper 1 m of the water column) was collected during high tide (i.e., salinity >32) on March 13th, 2016, pre-screened (200 μm mesh) to remove large zooplankton and put into acid-cleaned (1 N HCl) buckets, and immediately taken to the laboratory at Estación de Fotobiología Playa Unión (EFPU, 10 min away from the sampling site). Once in the laboratory, the original water sample was distributed in 12 ultraviolet (UVR)-transparent containers – microcosms (10-L capacity; LDPE Cubitainers, Nalgene) which represented three clusters of experimental scenarios (i.e., quadruplicates) as follows: A) Present (Pres): four microcosms filled with

seawater without any modification i.e., ambient environmental conditions (controls). B) Future "inside" (Fut_{in}): four microcosms filled with seawater that was acidified, and nutrients and DOM added (see below); and C) Future "outside" (Fut_{out}): four microcosms filled with seawater with the acidification and nutrients additions being similar as in the Fut_{in} but the DOM was outside the microcosms (see below).

The controls (Pres) had a pH of 8.3 and the initial concentration of macronutrients were 2.7 (SD = 0.7) μM phosphate, 2.4 (SD = 0.8) μM nitrite + nitrate, and 20.2 (SD = 6.1) μM silicate. In the Fut_{in} the seawater was acidified to the level predicted for 2100 (IPCC, 2013) to reach a pH = 7.6, achieved by the addition of CO_3^{2-} (as Na_2CO_3), HCO_3^- (as $NaHCO_3$) and HCl (0.1 N) to increase the pCO_2 and the dissolved inorganic carbon (DIC) (Gattuso et al., 2010). Macronutrients (i.e., phosphate as Na_2HPO_4, nitrate as $NaNO_3$, and silicate as Na_2SiO_3) were added to mimic an increase of their inputs from the Chubut River. The amount of nutrients added was based on a comparison between present and historical data of the Chubut River estuary (Bermejo et al., 2018) in which a general increase was observed in the inputs of nutrients due to anthropogenic activities. The nutrient concentrations in the Fut_{in} microcosms at the beginning of the experiment (after these additions) were 11.6 (SD = 3.1) μM phosphate, 61.4 (SD = 7.1) μM nitrite + nitrate, and 32 (SD = 2.9) μM silicate. In this experimental treatment the river terrigenous material was treated (see below) and added to the microcosms doubling the initial dissolved organic carbon (DOC) concentration (see below); this concentration of DOC was in turn, considered as an estimation of the DOM added. Therefore, and for simplicity, we will refer to this suspension of terrigenous material as to DOM, even though some particles and/or inorganic material might be included due to the technique used to extract it.

The Fut_{out} microcosms had the same initial acidification and nutrients additions as in the Fut_{in} but had a slightly lower nutrient concentrations (although not significantly different from that in the Fut_{in}) i.e., 10.1 (SD = 1.4) μM phosphate, 59.5 (SD = 2.6) μM nitrite + nitrate, and 31.7 (SD = 5) μM silicate. The DOM, however, was added to UVR-transparent bags (Alpax Trade Lab, São Paulo, Brazil, 72% transmission at 280 nm) that contained 4 L of filtered seawater; these bags were then put over the microcosms. The amount of DOM was such that the penetration of solar radiation in the microcosms was similar than that in the Fut_{in}.

We added controls (in triplicate) to evaluate the potential effects of pH or of solar radiation i.e., by degrading or altering the added DOM. We also used these controls to determine if some small phytoplankton cells were added to the microcosms together with the DOM. The controls were prepared as follows: Seawater was filtered through Munktell MG/F filters (25 mm diameter) and put into nine 500 mL-Teflon (UVR transparent) bottles, and the terrigenous mixture was added to reach the same DOC concentration as in the Fut_{in} (see below). Three different controls were done: 1) controls exposed to full solar radiation (photosynthetic available radiation (PAR + UVR, >280 nm), bottles uncovered, pH = 8.3; 2) controls exposed to full solar radiation (PAR + UVR, bottles uncovered) under increased acidity (pH = 7.6) and; 3) controls exposed to PAR (>400 nm, bottles wrapped with Ultraphan (UV 395 Opak Digefra film) under increased acidity (pH = 7.6). The controls were put in the water baths next to the microcosms and were gently shaken during daylight hours. On daily basis, sub-samples (50 mL) were taken for measurements of pH, and for the determination of chlorophyll-*a* (Chl-*a*) and absorption characteristics of the DOM (see below). There were no changes in the concentration of Chl-*a* in the controls (mean = 0.55 (SD = 0.09) μg Chl-*a* L^{-1}) suggesting that if small autotrophic cells were indeed added with the DOM, they were in very low quantity and they did not grow. In addition, there were no changes in the absorption of DOM (and therefore in the amount of DOC) in the controls during the time frame of our experiment.

All microcosms (and controls) were placed inside water baths to keep the in situ temperature (17 °C) and exposed to full solar radiation for 5 days, from 14th to 18th March 2016. The microcosms were gently shaken during daylight hours to avoid the settlement of cells and also to warrant homogeneous irradiance inside. Every day, before sunrise, subsamples (1 L) were taken from each microcosms, and part of this water (30 to 200 mL) was used for the determination of Chl-*a*, while ca. 30 mL were used to determine the absorption characteristics of the DOM added (see below). The pH in the microcosms was checked daily (using 50 mL of sample) and adjusted, when necessary, to reach the target value in the Future conditions of 7.6. At the beginning of the experiment (day 1), at the middle point (day 3) and at the end (day 5), subsamples were also collected from the microcosms for counting and identification of phytoplankton cells (125 mL), and for nutrients analyses (100 mL, see below). In addition, sub-samples were also used for oxygen (40 mL) and chl-*a* fluorescence measurements (100 mL).

2.3. Solar radiation measurements

Solar radiation was continuously monitored using a European Light Dosimeter Network broadband filter radiometer (ELDONET, Real Time Computers, Germany) that measures UV-B (280–315 nm), UV-A (315–400 nm), and PAR (400–700 nm) every second, averages the data over a 1-min interval, and stores them in a computer. This radiometer is routinely calibrated (once a year) using a solar calibration procedure. For this calibration, the irradiance data during a clear sky condition was compared with the output of radiation transfer models such as STAR (Ruggaber et al., 1994) and Daylight (Björn and Murphy, 1985).

2.4. Nutrients and pH

The concentration of nutrients in the samples was measured by standard techniques (Strickland and Parsons, 1972) using a spectrophotometer (Hewlett Packard model HP 8453E, USA). Measurements of pH in the microcosms and in the controls were done early in the morning to determine variations during the day using a pH-meter (Hanna, model HI-2211, USA).

2.5. Source and handling of DOM

The DOM added to the Future treatments was prepared as follows: A sample of the upper 2 cm layer of sediments from the Chubut River bed was collected using a beaker. The sample was taken to the laboratory, diluted with filtered seawater (Munktell MG/F filters, 25 mm) and particles were allowed to settle for 30 min. The supernatant of this mixture was added to the Future treatments to increase the DOM amount inside the microcosms in the Fut_{in}, and outside (in a bag) in the Fut_{out} treatments. To determine the amount of DOM added to the microcosms, sub-samples from the supernatant were filtered through precombusted Munktell MG/F filters (25 mm) and the absorption spectra from 250 to 750 nm were obtained for the filtered fraction using a scanning spectrophotometer (Hewlett Packard model HP 8453E, USA). The absorption coefficient at 320 nm (in m^{-1}) was used as an estimator of the amount of DOM in the samples which was calculated following the equations of Osburn and Morris (2003) as:

$$a_{DOM}\ (m^{-1}) = OD_{320nm} * 2.303/l \quad (1)$$

where OD_{320nm} is the optical density measured with the spectrophotometer, and l is the cuvette path length (0.01 m).

Preliminary tests with the initial seawater sample and with the supernatant of the terrigenous material allowed us to calculate the amount needed (10 mL) to add to each microcosms to approximately double the DOC concentration in the Future treatments. A rough estimation of the amount of DOC (in g C m^{-3}) based on the a_{DOM} (in m^{-1}) was calculated after Morris et al. (1995) as:

$$DOC\ (g\ C\ m^{-3}) = a_{DOM}\ (m^{-1}) * 0.51 \quad (2)$$

2.6. Counting and identification of phytoplankton cells

Samples for the identification and counting of phytoplankton cells (> 2 μm i.e., nano- and microplankton) were placed in brown glass bottles and fixed with buffered formalin (final concentration 0.4% of formaldehyde in the sample). Sub-samples of 10–25 mL were allowed to settle for 24 h in a sedimentation chamber (Hydro-Bios GmbH, Germany). A drop of Rose Bengal was added to the chamber to better distinguish (small) cells from detritus / sediment, and species were identified and enumerated using an inverted microscope (Leica model DM IL, Germany) following the technique described by Villafañe and Reid (1995). The biovolumes of the phytoplankton cells were calculated according to Hillebrand et al. (1999) and then converted into carbon content (i.e., biomass) using the equations of Strathmann (1967), considering the abundance of cells in the samples.

The specific growth rates (μ) in each treatment were calculated based on phytoplankton carbon using either the total phytoplankton carbon concentration, the carbon content in the microplankton (20–200 μm) and nanoplankton (2–20 μm) sizes, or that of the two main taxonomic groups (i.e., diatoms and flagellates) as:

$$\mu = \ln (N_1/N_0)/(t_1 - t_0) \quad (3)$$

where N_0 and N_1 represent the initial and final carbon concentration of phytoplankton at the initial time (t_0) and that at the end (t_1) of the sampling period.

2.7. Chlorophyll-a (Chl-a) concentration

Samples to determine Chl-*a* concentration were collected daily from the microcosms and from the controls. Aliquots of 30–200 mL of sample were filtered onto Munktell MG-F glass fiber filters (25 mm) and put in 15 mL centrifuge tubes with 5 mL of absolute methanol to extract the photosynthetic pigments (Holm-Hansen and Riemann, 1978). The tubes containing the filters were then placed in a sonicator for 20 min at 20 °C, and the extraction was completed after 40 min more in darkness. After 1 h of extraction and 10 min of centrifugation at 2000 rpm (900*g*), the supernatant was used to determine the Chl-*a* concentration fluorometrically (Holm-Hansen et al., 1965). The fluorometer (Turner Designs, Trilogy, USA) is routinely calibrated against spectrophotometric measurements.

2.8. Photosystem II (PSII) photochemistry

Sub-samples from each microcosms were placed in 50 mL quartz tubes, and exposed to solar radiation in a water bath under the in situ temperature and under two radiation conditions i.e., PAB (>280 nm, uncovered tubes), and P (>400 nm, tubes covered with UV 395 Opak Digefra film) (total of 24 tubes, quadruplicates for each condition) during the daylight period (7:00 to 18:00 h). Sub-samples (2 mL) were taken every hour from the quartz tubes with a syringe to measure fluorescence parameters, using a portable pulse amplitude modulated (PAM) fluorometer (Walz, model Water-ED PAM, Germany). Six measurements were done on each sub-sample immediately after being collected, with each measurement lasting 10 s; therefore the total time for measuring each sample was 1 min, without any dark-acclimation period. The effective photochemical quantum yield (Φ_{PSII}) was calculated using the equations of Genty et al. (1990) and Weis and Berry (1987) as:

$$\Phi_{PSII} = \Delta F/F'm = (F'm - Ft)/F'm \quad (4)$$

where F′m is the maximum fluorescence in the light-exposed cells induced by a saturating light pulse (ca. 5300 μmol photons m^{-2} s^{-1} in 0.8 s) and Ft the current steady state fluorescence induced by an actinic light (492 μmol photons m^{-2} s^{-1} – peak at 660 nm) in light-adapted cells. The rate of electrons transported through the PSII (rETR, in μmol photons m^{-2} s^{-1}) i.e., an estimation of the photosynthetic rate, was calculated every hour from the values of Φ_{PSII} as:

$$rETR = \Phi_{PSII} * E_{PAR} * 0.5 \quad (5)$$

where Φ_{PSII} is the effective photochemical quantum yield, E_{PAR} is the PAR energy received by the phytoplankton cells, and 0.5 is a correction factor as half of the absorbed light energy is diverted to the PSII (Suggett et al., 2010). Daily integrated rETRs were calculated for days 1, 3, and 5 for each experimental condition, integrating the area under the rETR vs. time curve.

2.9. Net community production rates (NCP)

Sub-samples were taken from the microcosms and placed in 40-mL UVR-transparent Teflon FEP narrow-mouth bottles (Nalgene, total of 24 bottles) and exposed to solar radiation under the PAB and P treatments (quadruplicates for each condition) inside a water bath and next to the microcosms. Oxygen concentration was measured using an optode-probe system (Minioxy-10 Presens GmbH, Germany) equipped with fiber optics and sensor-spots (SP-PSt3-NAU-D5-YOP) together with the Oxyview 6.02 software to register the data. The system was calibrated before the measurements using a two-point calibration for 100% and 0% oxygen saturation, at the desired temperature and at atmospheric pressure. Oxygen concentration measurements were done every hour during the daylight period, in parallel with PSII measurements. NCP rates were determined as the slope of the linear regression of the oxygen concentration, normalized by phytoplankton carbon content (see below) vs. time, and expressed as mg O_2 $(mg\ C)^{-1}$ h^{-1}.

2.10. Data treatment and statistics

As there were no changes (one-way RM-ANOVA) in the amount of DOM (i.e., estimated as DOC concentration) along the experimental period for each scenario (i.e., Pres, Fut_{in} and Fut_{out}; $p > 0.05$ in all cases) the data were pooled and a mean (and SD) was calculated for each experimental scenario. One-way ANOVA was used to compare DOC concentration among the three scenarios, with a subsequent LSD test (Zar, 1999). The same analysis was used to establish differences in the specific growth rates of the community among the three experimental scenarios. A two-way ANOVA was used to determine differences in specific growth rates of the two main taxonomic groups (i.e., diatoms and flagellates) and in the community size structure (i.e., microplankton, 20–200 μm, and nanoplankton, 2–20 μm) among the three experimental scenarios.

Two-way repeated measures ANOVAs (RM-ANOVA) were used to determine differences in NCP rates and in daily integrated rETR as a function of the solar radiation treatment (i.e., PAB and P) among the three experimental scenarios, for the different acclimation periods (i.e., days 1, 3 and 5). When significant differences were detected, a post hoc LSD test was performed. The data used for the two-way RM-ANOVAs met the homoscedasticity criteria (using the Cochran, Hartley & Bartlett test) but not the normality (by Kolmogorov–Smirnov). Nevertheless, for large experiments (various treatments and replicates) the ANOVA is considered robust to the lack of normality (Underwood, 1997). In addition, the data was tested for sphericity (Mauchley Sphericity test) and adjusted using the Greenhouse-Geisser correction. Significant differences between the samples exposed to different treatments were established using a 95% confidence limit (Zar, 1999).

3. Results

3.1. Initial conditions of the sampling site/experimental microcosms

The surface water temperature at the time of sampling was 17 °C, the pH 8.3 and the salinity 32.4. At the beginning of the experiment,

the mean Chl-*a* concentration was 6.45 μg L^{-1} (SD = 0.44) and the community was dominated (>80% of the total abundance) by unidentified nanoplanktonic flagellates i.e., ~1800 cells mL^{-1}. Nanoplanktonic diatoms (mostly *Thalassiosira* sp. forming-chains (10–20 μm in diameter) accounted for the rest of the community (i.e., ~320 cells mL^{-1}) with a few microplankton species present e.g., *Thalassiosira* spp. and *Odontella aurita*. The abundance of dinoflagellates was negligible (<1% of total abundance) throughout the experiment; small grazers were not observed in any of the samples.

During the experimental period, the mean daily PAR irradiance received by the cells was 174 (SD = 5.5) W m^{-2} (equivalent to 800 (SD = 25.3) μmol photons m^{-2} s^{-1}) while the mean irradiances for UV-A and UV-B were 21.1 (SD = 0.8) and 0.6 (SD = 0.02) W m^{-2}, respectively. The concentration of DOC (Fig. 1) was significantly different ($p = 0.0004$) among the experimental scenarios, with the values in the Fut_{in} being significantly higher (mean = 8.6 g C m^{-3}, SD = 0.98) that those in the Pres and Fut_{out} (mean of 4.8 g C m^{-3} (SD = 0.79) and of 4.8 g C m^{-3} (SD = 1.09), respectively) throughout the experimental period. In addition, there were no significant differences ($p = 0.59$) in the DOC concentration among the three controls during the experimental period that had an overall mean value of 8.7 g C m^{-3} (SD = 0.6). This suggests a lack of individual or combined effects of UVR and acidification on the amount of DOM (estimated as DOC concentration) during the experiment.

3.2. Growth and changes in the community structure

The specific growth rates of the whole community were significantly different ($p = 0.001$) among the experimental scenarios, being the lowest in the Pres (mean = 0.31 d^{-1}, SD = 0.13) and the highest in the Fut_{out} (mean = 0.79 d^{-1}, SD = 0.02); Fut_{in} had intermediate values (mean = 0.54 d^{-1}, SD = 0.03) (Fig. 2A). The μ based on Chl-*a* determinations and cell counts (data not shown) had a clear correspondence with those obtained based on phytoplankton carbon biomass (Fig. 2A). The two main taxonomic groups, diatoms and flagellates, showed similar μ within each treatment (Fig. 2B); therefore their relative proportions (flagellates to diatoms) did not change throughout the experiment. By the end of the experiment, the community composition was rather similar to that at the beginning; however, slight differences were observed among the three scenarios, with a few large diatom species (e.g., *Thalassiosira* spp., *Guinardia* sp., *O. aurita*, *Dactyliosolen fragilissimus*) contributing to the total abundance in the Pres, whereas in the Fut_{in} the nanoplanktonic *Thalassiosira* spp., and small pennate

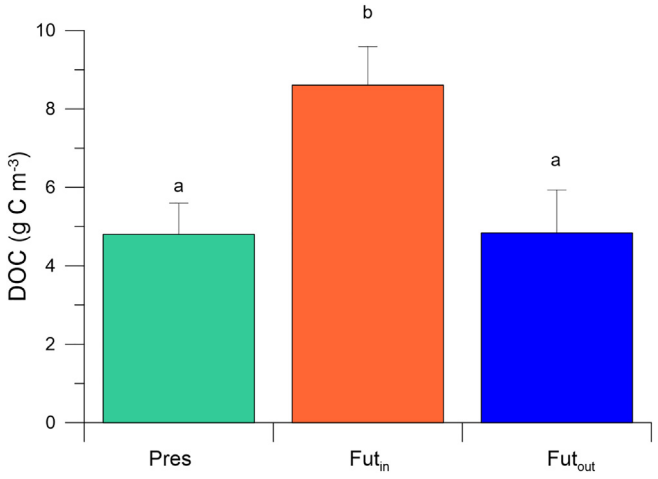

Fig. 1. Mean DOC concentration (an estimation of the amount of DOM in the microcosms) under the three experimental scenarios (i.e., Pres, Fut_{in} and Fut_{out}) during the timeframe of our experiment. The letters on top of the bars indicate the results of a post-hoc LSD test, after a one-way ANOVA, with the different letters indicating significant differences. The lines on top of the bars indicate the standard deviation (n = 4).

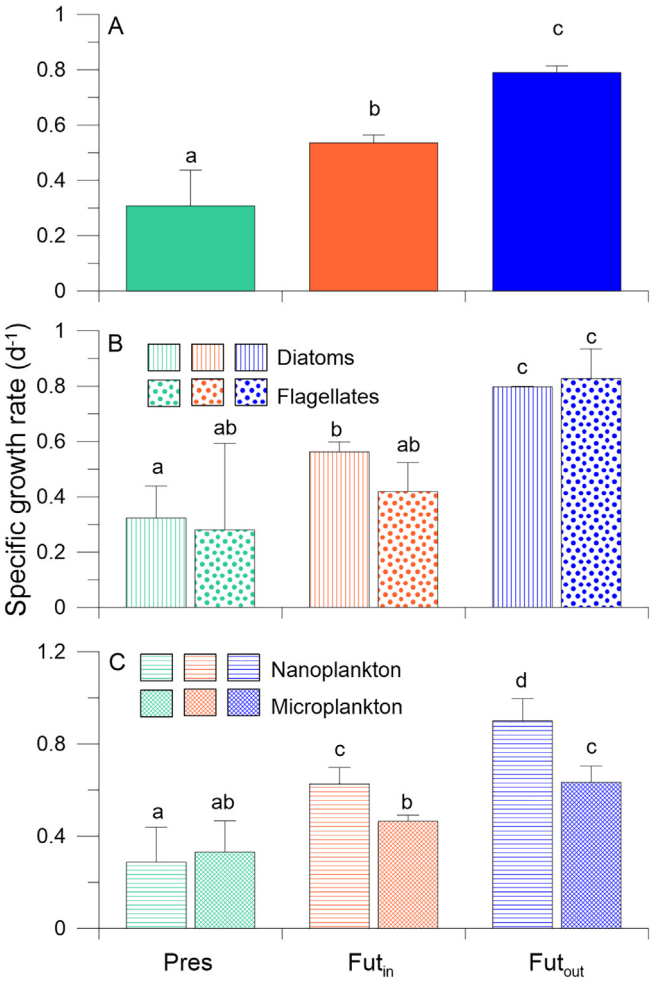

Fig. 2. Mean specific growth rates (in d^{-1}), and SD (n = 4) of phytoplankton in the three experimental scenarios - Pres, Fut_{in} and Fut_{out} of: A) total phytoplankton community; B) diatoms and flagellates and; C) microplankton (>20 μm) and nanoplankton (2–20 μm). The letters on top of the bars indicate the results of LSD post-hoc tests, after a one-way ANOVA (A) or two-way ANOVA (B and C), with the different letters indicating significant differences.

diatoms were the most abundant diatoms. On the other hand, in the Fut_{out}, the only relevant diatom species were nanoplanktonic *Thalassiosira* spp. However, the different experimental scenarios induced changes in the phytoplankton community size structure ($p = 0.004$, Fig. 2C): Microplankton had significantly higher μ in the Fut_{out} than in the Fut_{in} and Pres scenarios. Nanoplankton had the highest μ in the Fut_{out} and the lowest in the Pres, with the μ in the Fut_{in} having intermediate values. Within each Future condition, the growth of nanoplankton was significantly higher than that of microplankton ($p = 0.001$) while in the Pres there were no significant differences.

3.3. Electron transport rates and oxygen dynamics

The daily cycles of the calculated relative electron transport rates (rETRs) and oxygen concentration (in mg L^{-1}) are shown in Fig. 3. The rETRs (Fig. 3A, B, C) were different throughout the experiment, depending on the scenario. Also, a clear pattern of relatively higher rETR at noon as compared with the morning and afternoon values was observed for all the days and scenarios/treatments. On day 1 (Fig. 3A), the lowest rETRs values were determined in the Fut_{in} whereas the highest were measured either in the Pres or Fut_{out} samples that received the whole solar radiation spectrum, especially during the period mid-morning to early afternoon. In general, the rETRs values were much higher on day 1 than on days 3 and 5, for any treatment and during

sunlight hours. On day 3 (Fig. 3B) the rETRs values were very similar among the experimental scenarios, except for the samples under the Fut_{out} (receiving UVR) that had the highest values. Finally, on day 5 (Fig. 3C) a rather similar pattern as determined on day 1 was observed, with samples either under the Pres or Fut_{out} having a relatively higher rETR around noon, as compared to those under Fut_{in}. Oxygen concentrations (Fig. 3D, E, F), within any specific day, and for all experimental scenarios increased in general during most of the day (at least until 15 h) as a result of the photosynthetic process. On day 1 (Fig. 3D) the concentration of oxygen was similar in all the scenarios/treatments, and increased continuously during the morning/early afternoon and then it was rather constant for the rest of the day. On days 3 (Fig. 3E) and 5 (Fig. 3F) oxygen concentration increased during most of the day, and remained constant in late hours of the afternoon. In these two days, the concentration of oxygen in the Pres (controls) was lower than the ones in both Future treatments.

Based on the previously shown daily responses, we calculated the daily integrated rETRs (i.e., the area under each curve in Fig. 3A, B, C) and we used these values as a proxy of daily production (Fig. 4). There was a significant decrease ($p < 0.001$) in the integrated rETRs as the experiment progressed with values at the end of the acclimation period that were ca. 50%, 44% and 38% of those at the beginning, for the Fut_{out}, Pres, and Fut_{in}, respectively. Overall, UVR had a significant (Table 1) increase of rETRs, but this was more obvious in the Fut_{out} (throughout the experiment) and in the Pres at the start of the experimentation (Fig. 4). There were significant interactions between experimental scenarios and acclimation time for these integrated rETRs measurements (Table 1), with samples in the Fut_{in} having lower rETRs than the other treatments at day 1. As the experiment progressed, samples in the Pres had similar values on days 3 and 5, while samples in the Fut_{in} had similar values at days 1 and 3, decreasing on day 5. In the case of the Fut_{out}, there was a continuous decrease of integrated rETRs from day 1 to day 5 (post-hoc table inserted in Fig. 4).

From the daily oxygen data (Fig. 3D, E, F) NCP rates were obtained (i.e., during the part of the day in which oxygen concentration was increasing) and these values were normalized by the phytoplankton carbon content (Fig. 5). The highest NCP rates (for any particular scenario) were observed at the beginning, but then they decreased significantly ($p < 0.05$) as the experiment progressed. There were significant interactions between acclimation time and experimental scenario (Table 2)

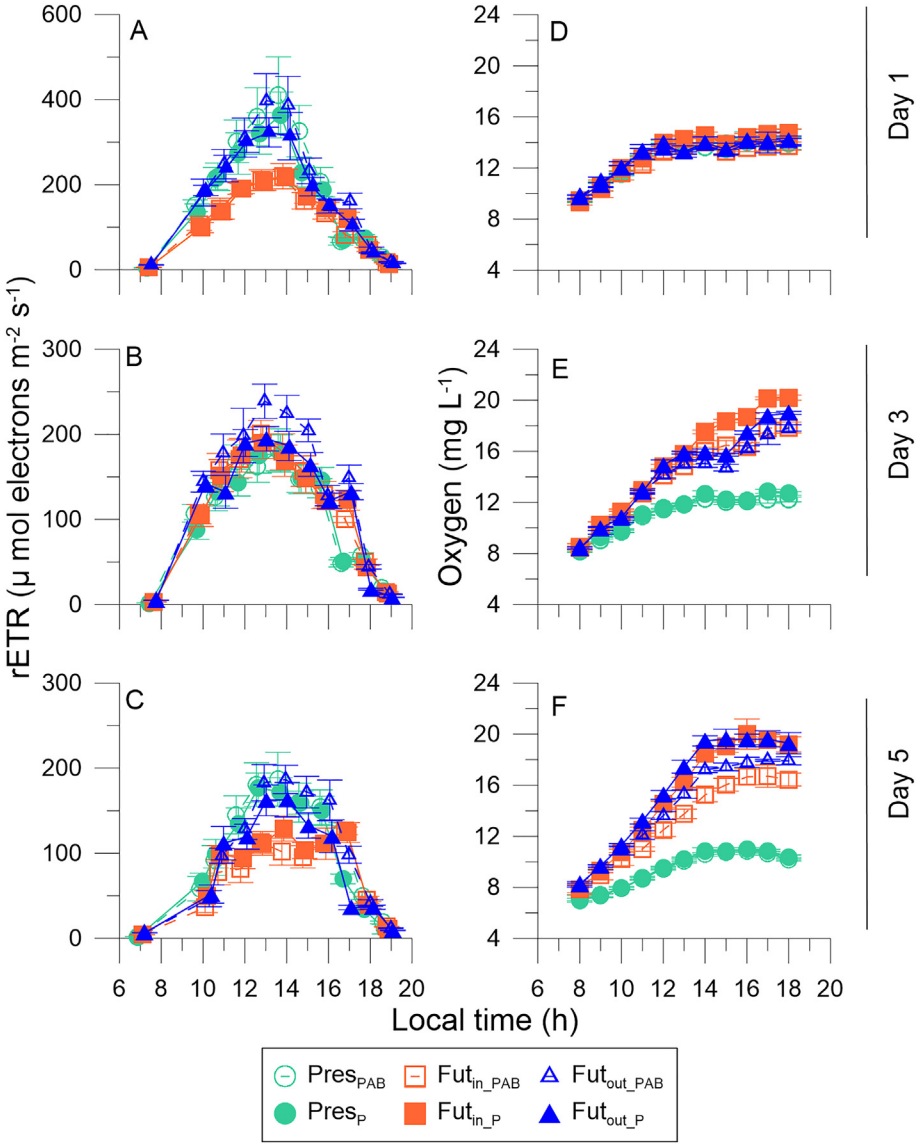

Fig. 3. Relative electron transport rates (rETRs, in µmol electrons m^{-2} s^{-1}) (A, B, C) and oxygen concentration (in mg L^{-1}) (D, E, F) throughout the day as a function of time: A, D) day 1; B, E) day 3, and; C, F) day 5, of samples acclimated to three experimental scenarios: Pres, Fut_{in} and Fut_{out}, and exposed to solar radiation under two treatments – PAB (UVR + PAR, >280 nm), and P (PAR, >400 nm. The vertical lines around the symbols indicate the standard deviation ($n = 4$).

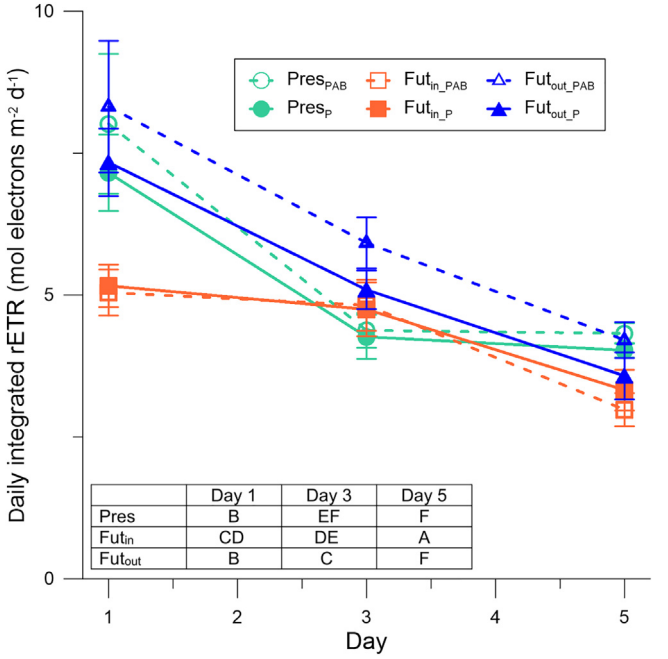

Fig. 4. Daily integrated rETRs (in mol electrons m^{-2} d^{-1}) under the three experimental scenarios (i.e., Pres, Fut_{in} and Fut_{out}) as a function of time, and exposure to solar radiation under two treatments – PAB (UVR + PAR, >280 nm), and P (PAR, >400 nm). The inserted table indicates the results of the LSD post-hoc test for the interaction between acclimation time and experimental scenario, after two-way repeated measures ANOVA, with different letters indicating significant differences. The vertical lines around the symbols indicate the standard deviation (n = 4).

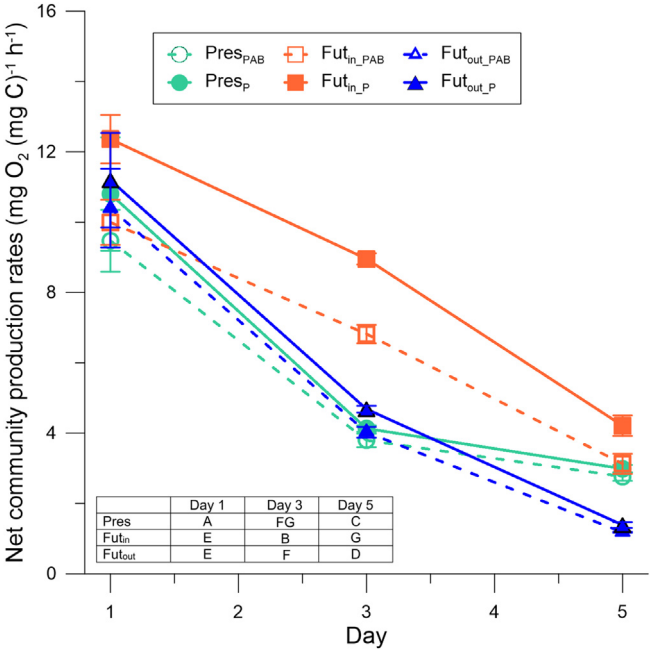

Fig. 5. Net community production rates, normalized by phytoplankton carbon content (in mg O_2 $(mg\ C)^{-1}$ h^{-1}) for the three experimental scenarios (i.e., Pres, Fut_{in} and Fut_{out}) as a function of time, and exposure to solar radiation under two treatments – PAB (UVR + PAR, >280 nm), and P (PAR, >400 nm). The inserted table indicates the results of the LSD post-hoc test for the interaction between acclimation time and experimental treatments, after two-way repeated measures ANOVA, with the different letters indicating significant differences. The vertical lines around the symbols indicate the standard deviation (n = 4).

with both Fut_{in} and Fut_{out} scenarios being significantly different from the Pres at the beginning of the experiment (day 1). By the end of the experiment (day 5) there were significant differences among the three scenarios, with the highest rates in the Fut_{in}, intermediates in the Pres and the lowest in the Fut_{out} (post-hoc table inserted in Fig. 5). There were also significant interactions between solar radiation and experimental scenario, but the amplitude of the impact of UVR decreasing NCP was especially evident in the Fut_{in} (Fig. 5).

We related both independent physiological data (i.e., NCP rates and the integrated rETRs) to obtain a measure of the effectiveness of the photosynthetic process under the three experimental scenarios (Fig. 6). Basically, we assessed how many moles of electrons (that will be used to form ATP and NADPH to be used later used in the Calvin-Benson-Bassham (CBB) cycle) passed through the PSII in relation to the amount of oxygen released after the water split (an estimation of the solar radiation absorbed). Within each experimental scenario the data were best adjusted using a linear relationship; there were no significant differences in the slope of the regressions between the PAB and P treatments for the Pres, Fut_{in} and Fut_{out}, so common regressions, including PAB and P, are shown in Fig. 6. The slope of the relationship between rETR and NCP rates varied however, with the scenario considered, being the lowest for the Fut_{in}, while the Pres and Fut_{out} had higher and similar slopes between them. In all the cases, the magnitude of the rETR/NCP ratio increased as the experiment progressed with the values at day 1 varying between 0.55 and 0.67 for the Fut_{in}, and between 0.9 and 1.2 and 0.9–1 for the Pres and Fut_{out}, respectively. At the end of the experiment (day 5) the values varied between 1.05 and 1.3, 1.8–2.1, and 3.3–4.7, for the Fut_{in}, Pres and Fut_{out} scenarios, respectively.

4. Discussion

The present work reports a lower rETR/NCP ratio in phytoplankton communities under global change conditions due to a physico-chemical, as compared only to a physical effect of DOM at mid-term time scales (Fig. 6). Conversely, these differences observed at subcellular level were not translated into different phytoplankton community structures that were dominated by nanoplanktonic species (Fig. 2). Nevertheless, in both Fut_{in} and Fut_{out} scenarios the growth of the community was significantly higher than in the Pres (Fig. 2A), with the highest μ values determined in the Fut_{out}, and with nanoplankton

Table 1
Results of the two-way RM-ANOVA for rETRs. Exp scen represents the three experimental scenarios (i.e., Pres, Fut_{in}, and Fut_{out}); Rad represents the solar radiation treatments (i.e., PAB, and P), and Acc time represents the three different days that were allowed the cells to acclimate to their experimental scenario.

	df	F	p
Exp scen	2	26.444	<0.001
Rad	1	5.199	<0.001
Exp scen * Rad	2	2.859	0.0836
Error	18		
Acc time	1.270552	265.896	<0.001
Acc time * Exp scen	2.541104	24.338	<0.001
Acc time * Radiat	1.270552	1.003	0.3475
Acc time * Exp scen * Rad	2.541104	0.525	0.6409
Error	22.869		

Table 2
Results of the two-way RM-ANOVA for NCP, where Exp scen represents the three experimental scenarios (i.e., Pres, Fut_{in}, and Fut_{out}); Rad represents the solar radiation treatments (i.e., PAB, and P), and Acc time represents the three different days that were allowed the cells to acclimate to their experimental scenario.

	df	F	p
Exp scen	2	78.689	<0.001
Rad	1	44.843	<0.001
Exp scen * Rad	2	7.831	<0.01
Error	18		
Acc time	1.058841	937.472	<0.001
Acc time * Exp scen	2.117683	21.841	<0.001
Acc time * Rad	1.058841	3.418	0.0781
Acc time * Exp scen * Rad	2.117683	0.448	0.6565
Error	19.059		

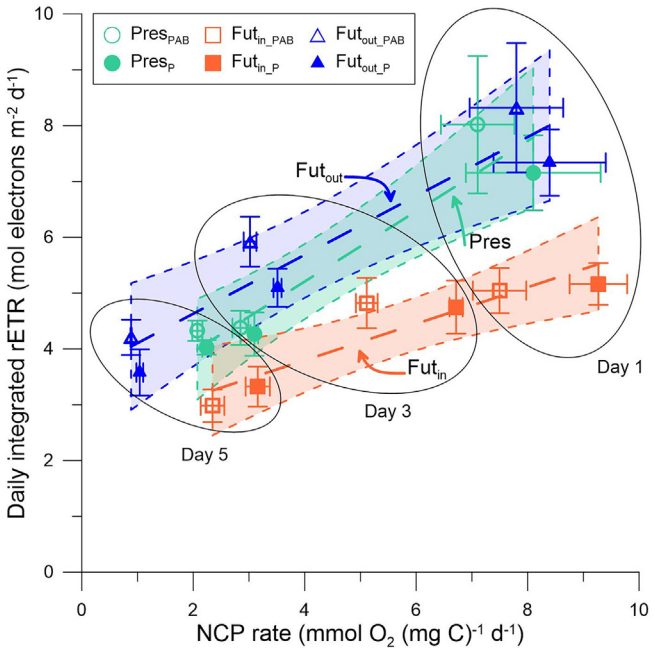

Fig. 6. Daily integrated rETRs (in mol electrons m^{-2} d^{-1}) as a function of the normalized NCP rates (in mmol O_2 (mg C)$^{-1}$ d^{-1}) in samples acclimated to the Pres, Fut_{in} and Fut_{out} experimental scenarios. The symbols are the mean values obtained on days 1, 3 and 5 and for the two radiation treatments – PAB and P. The vertical and horizontal lines around each symbol indicate the standard deviation (n = 4). The shaded areas represent the 95% confidence limits for the regression lines.

species having higher growth than microplankton (Fig. 2C). Although the effects of reduced pH on phytoplankton growth are not universal, part of the observed response in our experiments agree with the fact that elevated pCO_2 could act as a "fertilizer" due to the low CO_2 affinity of RUBISCO and the existence of carbon concentrating mechanisms (Grear et al., 2017). Also, even though the addition of nutrients could have benefited both Future conditions in terms of growth, they were not still fully utilized in the Pres treatment that at the end of the experiment they had a mean concentration of 1.8, 2.99, and 0.56 μM, for phosphate, silicate and nitrate + nitrite, respectively, suggesting that they were not limiting. Thus, processes other than the addition of nutrients were also involved in the increased overall growth of cells in the Future as compared to the Pres scenarios. The two Future scenarios received less radiation due to the physical attenuation of the DOM (Fig. 1) and this seemed to affect the growth of the community (Fig. 2A). However, when evaluating the growth of diatoms and flagellates (Fig. 2B) or the size structure of the community (Fig. 2C), small cells were those that grew more, but there were no differences between the Pres and Fut_{in} scenarios. It was expected, on the one hand, that large cells with a low surface-to-volume ratio would benefit from an increase in nutrients (Cotner and Biddanda, 2002); on the other hand, small cells, with a large surface-to-volume ratio would take advantage over large cells when the radiation decreases (Falkowski, 1981; Sarthou et al., 2005). Similarly, high pCO_2 causes shifts in the size abundance distributions of phytoplankton communities, often promoting the growth of small cells (Grear et al., 2017). In our experiments the balance between the two roles of DOM (i.e., as a source of nutrients or as an absorber of solar radiation) leans towards their physical role as a darker environment benefited the growth of nanoplanktonic cells (Fig. 2C). Indeed, the role of DOM as a protection against high solar radiation levels is very well known (Williamson and Rose, 2010) as seen, for example in sea-ice phytoplankton from the Baltic Sea (Piiparinen et al., 2015). Instead, the physico-chemical role of DOM could end in inhibiting the growth of cells in our experiments, probably due to toxic-induced effects of DOM (Meems et al., 2004; Timofeyev et al., 2004). It is already known that exposure to solar radiation accelerates the transformation of DOM into molecules that can be more readily used by organisms (Laurion and Mladenov, 2013) favoring the abundance of nanoflagellates (Forsström et al., 2013). This process however, was not observed in our study, as there was neither a significant change in the amount of DOM in any of the scenarios (Fig. 1) nor in the controls (data not shown). This suggests that more time or higher levels of solar radiation were needed to cause a significant photobleaching/photolysis of DOM (Osburn and Morris, 2003), a fact that was also observed in lakes and ponds (Laurion and Mladenov, 2013) and marine environments (Yamashita et al., 2013). However, if these changes indeed occurred, they were so small that they were not detected in the a_{320} parameter. We cannot rule out however, that even though we did not determine changes in the amount of DOM, there might have been temporal changes in the composition of the DOM (i.e., quality) as determined in other studies (Jaffé et al., 2008).

The relative importance of the physical vs. physico-chemical roles of DOM in a future global change scenario was also significantly different when addressing the short-term impact on the photosynthetic process (Fig. 6). Samples in the Fut_{out} and Pres treatments had a similar NCP (Fig. 3) and daily integrated ETR (Fig. 5) resulting in a similar trend rETR (i.e., the amount of electrons transported through the PSII) vs. oxygen rates (Fig. 6) throughout the experiment; in the Fut_{in}, on the other hand, they had a significantly lower trend. Thus higher oxygen rates were observed for a similar rETR (Fig. 6) suggesting a lower photosynthetic efficiency in the phytoplankton assemblage under the Fut_{in} scenario as compared to the Pres or Fut_{out}. One possible explanation, is that some of the unidentified flagellates (Fig. 2) could be mixotrophic, and thus under reduced incident radiation and increased organic C due to DOM (i.e., doubled respect Pres and Fut_{out} scenarios, Fig. 1) would alter their metabolism. They would change from being mostly photosynthetic obtaining C and energy (i.e., via photosynthesis) towards a more heterotrophic condition where (organic) C could be directly obtained through bacteria by phagotrophy (Wilken et al., 2018) and thus, light uptake was used to only obtain energy not C (Wilken et al., 2014). This dual strategy combining photo- and phagotrophy could sustain at least part of the mismatch observed between Fut_{in} vs. Fut_{out} (and Pres) in which only the C content of microcosms was manipulated. On the other hand, this potential higher phagotrophy could clearly be supported by the fact that increased nutrients and acidification also boosted bacterial production respect to present scenarios in the study area (Durán-Romero et al., 2017) hence these nanoflagellates could combine both metabolic as a strategy to cope with the stressful conditions experienced under the Fut_{in} scenario. Also, in the Fut_{in} treatment, the higher absorption of solar energy and consequently more water split (i.e., more oxygen) might have resulted in the formation of more free radicals (Kieber et al., 2003; Häder et al., 2015) as compared to the other scenarios. Thus the cells might have to cope with increasing ROS in detriment of other metabolic processes. Even more, the complexation of micronutrients with DOM could have reduced the availability of certain elements (i.e., iron) thus limiting primary productivity (Wells and Trick, 2004). However, the differences observed in the photosynthetic process among the scenarios were smaller towards the end of the experiment, with even higher efficiency in all scenarios (Fig. 6) suggesting an overall acclimation of the cells during the experimental period. Previous studies carried out in the study area have shown that 5 days was enough for phytoplankton cells to acclimate to the conditions imposed in the experiments, and this was seen in the synthesis of antioxidants (Janknegt et al., 2009) and of UV-absorbing compounds (Marcoval et al., 2007; Helbling et al., 2008), in the activation of the xanthophyll cycle (van de Poll et al., 2010), in the increase of RUBISCO and gene expression (Helbling et al., 2011) as well as in changes in the species composition and thus in the community response (Villafañe et al., 2015; Durán-Romero et al., 2017).

Finally, it is interesting to note the differential effects of radiation quality observed in our experiments. On the one hand, the differences between radiation treatments observed in the daily integrated rETRs,

with significantly higher values in those samples exposed to the full radiation spectrum (Fig. 4) hints for a beneficial effect of UVR on the photosynthetic process, as also seen in our study area (Barbieri et al., 2002) as well as in tropical sites (Helbling et al., 2003). However, such positive effect of this waveband was not observed in the NCP rates (Fig. 5) in which UVR clearly reduced oxygen production, especially in the Fut_{in} scenario. These apparently contrasting effects of UVR have been observed in previous studies (Helbling et al., 2011) and they were attributed to the fact that it affects differently the diverse targets of photosynthesis (i.e., water split, electronic transport through PSII, carbon incorporation). This is also true for other variables than UVR, such that the different targets are more vulnerable (or resistant) when exposed to e.g., lower pH, as seen in the green alga *Ulva* (Xu and Gao, 2012).

Overall, our study suggests that in future simulated conditions of global change, with higher amount of nutrients and acidity, the increasing amount of terrigenous material (e.g., DOM) would benefit small nanoplanktonic species mainly due to a reduction of the solar radiation levels (i.e., UVR) received by the cells (i.e., physical role of the DOM). DOM, however, might also react with solar radiation generating an additional stress to the cells, thus counteracting somehow the beneficial "physical role", leading us to reject our initial hypothesis. Our results are in agreement with recent observations (Bais et al., 2018) that suggests that overall, absorption by DOM of solar UVR reduces DNA damage more than indirect chemical reactions increase the damage. However, the acclimation of cells also plays an important role and need to be taken into consideration as the initial impact of future simulated conditions decrease with time and cells are more effective utilizing solar energy in the photosynthetic process. Overall, the knowledge of the relative importance of the physical and chemical roles of DOM in a future scenario will be especially important for coastal areas that are expected to receive higher inputs of DOM.

Acknowledgments

We thank M. Cabrerizo for his help with computer drawings. This work was supported by Agencia Nacional de Promoción Científica y Tecnológica - ANPCyT (PICT 2013-0208 and PICT 2015-0462), the Swedish Secretariat for Environmental Earth System Sciences (SSEESS) – The Royal Swedish Academy of Sciences, the Swedish Research Programme EcoChange, Consejo Nacional de Investigaciones Científicas y Técnicas (CONICET) and Fundación Playa Unión. We thank Cooperativa Eléctrica y de Servicios de Rawson for providing building infrastructure for carrying out these experiments. We thank the comments and suggestions of three anonymous reviewers that helped us to improve our Ms. This is Contribution N° 172 of Estación de Fotobiología Playa Unión.

References

Bais, A.F., Lucas, R.M., Bornman, J.F., Williamson, C.E., Sulzberger, B., Austin, A.T., Wilson, S. R., Andrady, A.L., Bernhard, G., McKenzie, R.L., Aucamp, P.J., Madronich, S., Neale, R.E., Yazar, S., Young, A.R., de Gruijl, F.R., Norval, M., Takizawa, Y., Barnes, P.W., Robson, T. M., Robinson, S.A., Ballaré, C.L., Flint, S.D., Neale, P.J., Hylander, S., Rose, K.C., Wängberg, S.-Å., Häder, D.-P., Worrest, R.C., Zepp, R.G., Paul, N.D., Cory, R.M., Solomon, K.R., Longstreth, J., Pandey, K.K., Redhwi, H.H., Torikai, A., Heikkilä, A.M., 2018. Environmental effects of ozone depletion, UV radiation and interactions with climate change: UNEP Environmental Effects Assessment Panel, update 2017. Photochem. Photobiol. Sci. 17, 127–179.

Barbieri, E.S., Villafañe, V.E., Helbling, E.W., 2002. Experimental assessment of UV effects upon temperate marine phytoplankton when exposed to variable radiation regimes. Limnol. Oceanogr. 47, 1648–1655.

Behrenfeld, M.J., Falkowski, P.G., 1997. Photosynthetic rates derived from satellite-based chlorophyll concentration. Limnol. Oceanogr. 42, 1–20.

Bermejo, P., Helbling, E.W., Durán-Romero, C., Cabrerizo, M.J., Villafañe, V.E., 2018. Abiotic control of phytoplankton blooms in temperate coastal marine ecosystems: a case study in the South Atlantic Ocean. Sci. Total Environ. 612, 894–902.

Björn, L.O., Murphy, T.M., 1985. Computer calculation of solar ultraviolet radiation at ground level. Physiol. Veg. 23, 555–561.

Cabrerizo, M.J., Carrillo, P., Villafañe, V.E., Medina-Sáchez, J.M., Helbling, E.W., 2017. Increased nutrients from aeolian-dust and riverine origin decrease the CO_2-sink capacity of coastal South Atlantic waters under UVR exposure. Limnol. Oceanogr. https://doi.org/10.1002/lno.10764 (in press).

Canuel, E.A., Cammer, S.S., McIntosh, H.A., Pondell, C.R., 2012. Climate change impacts on the organic carbon cycle at the land-ocean interface. Annu. Rev. Earth Planet. Sci. 40, 685–711.

Cloern, J.E., Foster, S.Q., Fleckner, A.E., 2014. Phytoplankton primary production in the world's estuarine-coastal ecosystems. Biogeosciences 11, 2477–2501.

Cloern, J.E., Abreu, P.C., Carstensen, J., Chauvaud, L., Elmgren, R., Grall, J., Greening, H., Johansson, J.O.R., Kahru, M., Sherwood, E.T., Xu, J.I.E., Yin, K., 2016. Human activities and climate variability drive fast-paced change across the world's estuarine–coastal ecosystems. Glob. Chang. Biol. 22, 513–529.

Cotner, B.J., Biddanda, B.A., 2002. Small players, large role: microbial influence on biogeochemical processes in pelagic aquatic ecosystems. Ecosystems 5, 105–121.

Crain, C.M., Kroeker, K., Halpern, B.S., 2008. Interactive and cumulative effects of multiple human stressors in marine systems. Ecol. Lett. 11, 1304–1315.

De Carli, P., Braccalenti, J.C., García-de-León, F.J., Acuña-Gómez, E.P., 2012. La pesquería del langostino argentino *Pleoticus muelleri* (Crustacea: Penaeidae) en Patagonia, ¿Un único stock? An. Inst. Patagonia 40, 103–112.

Durán-Romero, C., Villafañe, V.E., Valiñas, M.S., Gonçalves, R.J., Helbling, E.W., 2017. Solar UVR sensitivity of phyto- and bacterioplankton communities from Patagonian coastal waters under increased nutrients and acidification. ICES J. Mar. Sci. 74, 1062–1073.

Falkowski, P.G., 1981. Light shade adaptation and assimilation numbers. J. Plankton Res. 3, 203–216.

Forsström, L., Roiha, T., Rautio, M., 2013. Responses of microbial food web to increased allochthonous DOM in an oligotrophic subarctic lake. Aquat. Microb. Ecol. 68, 171–184.

Gattuso, J.P., Gao, K., Lee, K., Rost, B., Schulz, K.G., 2010. Approaches and tools to manipulate the carbonate chemistry. In: Riebesell, U., Fabry, V.J., Hansson, L., Gattuso, J.-P. (Eds.), Guide to Best Practices for Ocean Acidification Research and Data Reporting. Publications Office of the European Union, Brussels, pp. 41–52.

Genty, B.E., Harbinson, J., Baker, N.R., 1990. Relative quantum efficiencies of the two photosystems of leaves in photorespiratory and non-photorespiratory conditions. Plant Physiol. Biochem. 28, 1–10.

Grear, J.S., Rynearson, T.A., Montalbano, A.L., Govenar, B., Menden-Deuer, S., 2017. pCO_2 effects on species composition and growth of an estuarine phytoplankton community. Estuar. Coast. Shelf Sci. 190, 40–49.

Häder, D.P., Villafañe, V.E., Helbling, E.W., 2014. Productivity of aquatic primary producers under global climate change. Photochem. Photobiol. Sci. 13, 1370–1392.

Häder, D.-P., Williamson, C.E., Wängberg, S.-A., Rautio, M., Rose, K.C., Gao, K., Helbling, E. W., Sinha, R.P., Worrest, R., 2015. Effects of UV radiation on aquatic ecosystems and interactions with other environmental factors. Photochem. Photobiol. Sci. 14, 108–126.

Helbling, E.W., Gao, K., Gonçalves, R.J., Wu, H., Villafañe, V.E., 2003. Utilization of solar ultraviolet radiation by phytoplankton assemblages from the Southern China Sea when exposed to fast mixing conditions. Mar. Ecol. Prog. Ser. 259, 59–66.

Helbling, E.W., Buma, A.G.J., Van de Poll, W., Fernández Zenoff, M.V., Villafañe, V.E., 2008. UVR-induced photosynthetic inhibition dominates over DNA damage in marine dinoflagellates exposed to fluctuating solar radiation regimes. J. Exp. Mar. Biol. Ecol. 365, 96–102.

Helbling, E.W., Pérez, D.E., Medina, C.D., Lagunas, M.G., Villafañe, V.E., 2010. Phytoplankton distribution and photosynthesis dynamics in the Chubut River estuary (Patagonia, Argentina) throughout tidal cycles. Limnol. Oceanogr. 55, 55–65.

Helbling, E.W., Buma, A.G.J., Boelen, P., van der Strate, H.J., Fiorda Giordanino, M.V., Villafañe, V.E., 2011. Increase in Rubisco activity and gene expression due to elevated temperature partially counteracts ultraviolet radiation–induced photoinhibition in the marine diatom *Thalassiosira weissflogii*. Limnol. Oceanogr. 56, 1330–1342.

Helbling, E.W., Banaszak, A.T., Villafañe, V.E., 2015. Global change feed-back inhibits cyanobacterial photosynthesis. Sci. Rep. 5 (14514). https://doi.org/10.1038/srep14514.

Hillebrand, H., Dürselen, C.D., Kirschtel, D., Pollingher, U., Zohary, T., 1999. Biovolume calculation for pelagic and benthic microalgae. J. Phycol. 35, 403–424.

Holm-Hansen, O., Riemann, B., 1978. Chlorophyll a determination: improvements in methodology. Oikos 30, 438–447.

Holm-Hansen, O., Lorenzen, C.J., Holmes, R.W., Strickland, J.D.H., 1965. Fluorometric determination of chlorophyll. J. Cons. Perm. Int. Explor. Mar. 30, 3–15.

IPCC, 2013. Climate Change 2013. The Physical Science BasisCambridge University Press, New York, USA 1535 pp.

Iriarte, J.L., Ardelan, M.V., Cuevas, L.A., González, H.E., Sanchez, N., Myklestad, S.M., 2014. Size-spectrum based differential response of phytoplankton to nutrient and iron-organic matter combinations in microcosm experiments in a Chilean Patagonian Fjord. Phycol. Res. 62, 136–146.

Jaffé, R., McKnight, D., Maie, N., Cory, R., McDowell, W.H., Campbell, J.L., 2008. Spatial and temporal variations in DOM composition in ecosystems: the importance of long-term monitoring of optical properties. J. Geophys. Res. 113, G04032.

Janknegt, P.J., De Graaff, M., Van de Poll, W., Visser, R.J., Helbling, E.W., Buma, A.G.J., 2009. Antioxidative responses of two marine microalgae during acclimation to static and fluctuating natural UV radiation. Photochem. Photobiol. 85, 1336–1345.

Johnson, M.S., Meskhidze, N., Kiliyanpilakkil, V.P., Gassó, S., 2011. Understanding the transport of Patagonian dust and its influence on marine biological activity in the South Atlantic Ocean. Atmos. Chem. Phys. 11, 2487–2502.

Jones, R.I., 1992. The influence of humic substances on lacustrine planktonic food chains. Hydrobiologia 229, 73–91.

Kieber, D.J., Peake, B.M., Scully, N.M., 2003. Reactive oxygen species in aquatic ecosystems. In: Helbling, E.W., Zagarese, H.E. (Eds.), UV Effects in Aquatic Organisms and Ecosystems. Royal Society of Chemistry, Cambridge, pp. 251–288.

Kim, J.-A., Lee, K., Shin, K., Yang, E.J., Engel, A., Karl, D.M., Kim, H.-C., 2011. Shifts in biogenic carbon flow from particulate to dissolved forms under high carbon dioxide and warm ocean conditions. Geophys. Res. Lett. 38 (L08612).

Kissman, C.E.H., Williamson, C.E., Rose, K.C., Saros, J.E., 2013. Response of phytoplankton in an alpine lake to inputs of dissolved organic matter through nutrient enrichment and trophic forcing. Limnol. Oceanogr. 58, 867–880.
Klug, J.L., 2002. Positive and negative effects of allochthonous dissolved organic matter and inorganic nutrients on phytoplankton growth. Can. J. Fish. Aquat. Sci. 59, 85–95.
Laurion, I., Mladenov, N., 2013. Dissolved organic matter photolysis in Canadian arctic thaw ponds. Environ. Res. Lett. 8, 035026.
Lindh, M.V., Lefébure, R., Degerman, R., Lundin, D., Andersson, A., Pinhassi, J., 2015. Consequences of increased terrestrial dissolved organic matter and temperature on bacterioplankton community composition during a Baltic Sea mesocosm experiment. Ambio 44, S402–S412.
Marcoval, M.A., Villafañe, V.E., Helbling, E.W., 2007. Interactive effects of ultraviolet radiation and nutrient addition on growth and photosynthesis performance of four species of marine phytoplankton. J. Photochem. Photobiol. B Biol. 89, 78–87.
Meems, N., Steinberg, C.E., Wiegand, C., 2004. Direct and interacting toxicological effects on the waterflea (*Daphnia magna*) by natural organic matter, synthetic humic substances and cypermethrin. Sci. Total Environ. 319, 123–136.
Morris, D.P., Zagarese, H.E., Williamson, C.E., Balseiro, E.G., Hargreaves, B.R., Modenutti, B. E., Moeller, R., Quemaliños, C.P., 1995. The attenuation of solar UV radiation in lakes and the role of dissolved organic carbon. Limnol. Oceanogr. 40, 1381–1391.
Osburn, C.L., Morris, D.P., 2003. Photochemistry of chromophoric dissolved organic matter in natural waters. In: Helbling, E.W., Zagarese, H. (Eds.), UV Effects in Aquatic Organisms and Ecosystems. Royal Society of Chemistry, Cambridge, pp. 185–217.
Piiparinen, J., Enberg, S., Rintala, J.M., Sommaruga, R., Majaneva, M., Autio, R., Vähätalo, A. V., 2015. The contribution of mycosporine-like amino acids, chromophoric dissolved organic matter and particles to the UV protection of sea-ice organisms in the Baltic Sea. Photochem. Photobiol. Sci. 14, 1025–1038.
van de Poll, W., Buma, A.G.J., Visser, R.J., Janknegt, P.J., Villafañe, V.E., Helbling, E.W., 2010. Xanthophyll cycle activity and photosynthesis of *Dunaliella tertiolecta* (Chlorophyceae) and *Thalassiosira weissflogii* (Bacillariophyceae) during fluctuating solar radiation. Phycologia 49, 249–259.
Rabalais, N.N., Turner, R.E., Díaz, R.J., Justic, D., 2009. Global change and eutrophication of coastal waters. ICES J. Mar. Sci. 66, 1528–1537.
Riebesell, U., 2004. Effects of CO_2 enrichment on marine phytoplankton. J. Oceanogr. 60, 719–729.
Rousseaux, C.S., Gregg, W.W., 2014. Interannual variation in phytoplankton primary production at a global scale. Remote Sens. 6, 1–19.
Ruggaber, A., Dlugi, R., Nakajima, T., 1994. Modelling of radiation quantities and photolysis frequencies in the troposphere. J. Atmos. Chem. 18, 171–210.
Santos, L., Pinto, A., Filipe, O., Cunha, Â., Santos, E.B.H., Almeida, A., 2016. Insights on the optical properties of estuarine DOM – hydrological and biological influences. PLoS One 11. https://doi.org/10.1371/journal.pone.0154519.
Sarthou, G., Timmermans, K.R., Blain, S., Tréguer, P., 2005. Growth physiology and fate of diatoms in the ocean: a review. J. Sea Res. 53, 25–42.
Scapini, M.C., Conzonno, V.H., Balzaretti, V.T., Fernández Cirelli, A., 2010. Comparison of marine and river water humic substances in a Patagonian environment (Argentina). Aquat. Sci. 72, 1–12.
Scapini, M.C., Conzonno, V., Orfila, J., Saravia, J., Balzaretti, V.T., Cirelli, A.F., 2011. Limnological aspects of humic substances in Chubut river (Patagonia-Argentina). River Res. Appl. 27, 1264–1269.
Skewgar, E., Boersma, P.D., Harris, G., Caille, G., 2007. Sustainability: anchovy fishery threat to Patagonian ecosystem. Science 315, 45.
Strathmann, R.R., 1967. Estimating the organic carbon content of phytoplankton from cell volume or plasma volume. Limnol. Oceanogr. 12, 411–418.
Strickland, J.D.H., Parsons, T.R., 1972. A Practical Handbook of Seawater Analysis. 167. Fish. Res. Board Can. Bull., pp. 1–310.
Suggett, D.J., Oxborough, K., Baker, N.R., MacIntyre, H.L., Kana, T.M., Geider, R.J., 2010. Fast repetition rate and pulse amplitude modulation chlorophyll *a* fluorescence measurements for assessment of photosynthetic electron transport in marine phytoplankton. Eur. J. Phycol. 38, 371–384.
Thornton, D.C.O., 2014. Dissolved organic matter (DOM) release by phytoplankton in the contemporary and future ocean. Eur. J. Phycol. 49, 20–46.
Timofeyev, M.A., Wiegand, C., Kent Burnison, B., Shatilina, Z.M., Pflugmacher, S., Steinberg, C.E., 2004. Impact of natural organic matter (NOM) on freshwater amphipods. Sci. Total Environ. 319, 115–121.
Traving, S.J., Rowe, O., Jakobsen, N.M., Sørensen, H., Dinasquet, J., Stedmon, C.A., Andersson, A., Riemann, L., 2017. The effect of increased loads of dissolved organic matter on estuarine microbial community composition and function. Front. Microbiol. 8. https://doi.org/10.3389/fmicb.2017.00351.
Underwood, A.J., 1997. Experiments in Ecology: Their Logical Design and Interpretation Using Analysis of Variance. Cambridge University Press (524 pp.).
UNEP, UNEP (Eds.), 2006. Marine and Coastal Ecosystems and Human Well-being: A Synthesis Report Based on the Findings of the Millennium Ecosystem Assessment, p. 76.
Villafañe, V.E., Reid, F.M.H., 1995. Métodos de microscopía para la cuantificación del fitoplancton. In: Alveal, K., Ferrario, M.E., Oliveira, E.C., Sar, E. (Eds.), Manual de Métodos Ficológicos. Universidad de Concepción, Concepción, Chile, pp. 169–185.
Villafañe, V.E., Valiñas, M.S., Cabrerizo, M.J., Helbling, E.W., 2015. Physio-ecological responses of Patagonian coastal marine phytoplankton in a scenario of global change: role of acidification, nutrients and solar UVR. Mar. Chem. 177, 411–420.
Weis, E., Berry, A., 1987. Quantum efficiency of photosystem II in relation to the energy dependent quenching of chlorophyll fluorescence. Biochim. Biophys. Acta 894, 198–208.
Wells, M.L., Trick, C.G., 2004. Controlling iron availability to phytoplankton in iron-replete coastal waters. Mar. Chem. 86, 1–13.
Wilken, S., Schuurmans, J.M., Matthijs, H.C.P., 2014. Do mixotrophs grow as photoheterotrophs? Photophysiological acclimation of the chrysophyte *Ochromonas danica* after feeding. New Phytol. 204, 882–889.
Wilken, S., Soares, M.O., Urrutia-Cordero, P., Ratcovich, J., Ekvall, M.K., Van Donk, E., Hansson, L.A., 2018. Primary producers or consumers? Increasing phytoplankton bacterivory along a gradient of lake warming and browning. Limnol. Oceanogr. 63, S142–S155.
Williamson, C.E., Rose, K.C., 2010. When UV meets freshwater. Science 329, 637–639.
Wilson, J.G., 2008. Adaptations to life in estuaries. In: Safran, P. (Ed.), Encyclopedia of Life Support Systems (EOLSS). EOLSS Publishers, Oxford, UK, pp. 166–180.
Xu, J., Gao, K., 2012. Future CO_2-induced ocean acidification mediates the physiological performance of a green tide alga. Plant Physiol. 160, 1762–1769.
Yamashita, Y., Nosaka, Y., Suzuki, K., Ogawa, H., Takahashi, K., Saito, H., 2013. Photobleaching as a factor controlling spectral characteristics of chromophoric dissolved organic matter in open ocean. Biogeosciences 10, 7207–7217.
Zar, J.H., 1999. Biostatistical Analysis. 4th ed. Prentice Hall, Englewood Cliffs, NJ (929 pp.).